HHS Public Access

Author manuscript

Int J Comput Assist Radiol Surg. Author manuscript; available in PMC 2017 August 01.

Published in final edited form as:

Int J Comput Assist Radiol Surg. 2016 August ; 11(8): 1475–1486. doi:10.1007/s11548-015-1344-5.

Corticospinal tract modeling for neurosurgical planning by tracking through regions of peritumoral edema and crossing fibers using two-tensor unscented Kalman filter tractography

Zhenrui Chen, MD,
Department of Neurosurgery, Brigham and Women's Hospital, Harvard Medical School, Boston, Massachusetts 02115

Department of Neurosurgery, Jinling Hospital, Southern Medical University, Nanjing, 210002, Jiangsu, China

Yanmei Tie, PhD,
Department of Neurosurgery, Brigham and Women's Hospital, Harvard Medical School, Boston, Massachusetts 02115

Olutayo Olubiyi, MBChB, MPH,
Department of Neurosurgery, Brigham and Women's Hospital, Harvard Medical School, Boston, Massachusetts 02115

Alireza Mehrtash, MSc,
Department of Neurosurgery, Brigham and Women's Hospital, Harvard Medical School, Boston, Massachusetts 02115

Department of Radiology, Brigham and Women's Hospital, Harvard Medical School, Boston, Massachusetts 02115

Laura Rigolo, MA,
Department of Neurosurgery, Brigham and Women's Hospital, Harvard Medical School, Boston, Massachusetts 02115

Isaiah Norton, BS,
Department of Neurosurgery, Brigham and Women's Hospital, Harvard Medical School, Boston, Massachusetts 02115

Ofer Pasternak, PhD,
Department of Radiology, Brigham and Women's Hospital, Harvard Medical School, Boston, Massachusetts 02115

Corresponding Authors: Alexandra J. Golby, MD, Department of Neurosurgery, Brigham and Women's Hospital, 75 Francis Street, Boston, MA 02115, agolby@bwh.harvard.edu, Telephone: 617-525-6776, Fax: 617-713-3050; Lauren J. O'Donnell, PhD, 1249 Boylston St., Room #210 Boston, MA 02215, odonnell@bwh.harvard.edu, Telephone: 617-875-3326.
*senior co-authors

Ethical standards statement: All procedures followed were in accordance with the ethical standards of the responsible committee on human experimentation (institutional and national) and with the Helsinki Declaration of 1975, as revised in 2008. The study was approved by the Partners Healthcare Institutional Review Board, and written informed consent was obtained from all subjects prior to participation.

Conflict of Interest: The authors declare that they have no conflict of interest.

Department of Psychiatry, Brigham and Women's Hospital, Harvard Medical School, Boston, Massachusetts 02115

Yogesh Rathi, PhD,
Department of Psychiatry, Brigham and Women's Hospital, Harvard Medical School, Boston, Massachusetts 02115

Alexandra J. Golby, MD*, and
Department of Neurosurgery, Brigham and Women's Hospital, Harvard Medical School, Boston, Massachusetts 02115

Department of Radiology, Brigham and Women's Hospital, Harvard Medical School, Boston, Massachusetts 02115

Lauren J. O'Donnell, PhD*
Department of Neurosurgery, Brigham and Women's Hospital, Harvard Medical School, Boston, Massachusetts 02115

Department of Radiology, Brigham and Women's Hospital, Harvard Medical School, Boston, Massachusetts 02115

Abstract

Purpose—The aim of this study was to present a tractography algorithm using a two-tensor unscented Kalman filter (UKF) to improve the modeling of the corticospinal tract (CST) by tracking through regions of peritumoral edema and crossing fibers.

Methods—Ten patients with brain tumors in the vicinity of motor cortex and evidence of significant peritumoral edema were retrospectively selected for the study. All patients underwent 3-Tesla magnetic resonance imaging (MRI) including functional MRI (fMRI) and a diffusion-weighted data set with 31 directions. Fiber tracking was performed using both single-tensor streamline and two-tensor UKF tractography methods. A two-regions-of-interest approach was used to delineate the CST. Results from the two tractography methods were compared visually and quantitatively. fMRI was applied to identify the functional fiber tracts.

Results—Single-tensor streamline tractography underestimated the extent of tracts running through the edematous areas and could only track the medial projections of the CST. In contrast, two-tensor UKF tractography tracked fanning projections of the CST despite peritumoral edema and crossing fibers. The two-tensor UKF tractography delineated tracts that were closer to motor fMRI activations, and it was more sensitive than single-tensor streamline tractography to define the tracts directed to the motor sites. The volume of the CST was significantly larger on two-tensor UKF than on single-tensor streamline tractography ($p < 0.001$).

Conclusions—Two-tensor UKF tractography tracks the CST better than single-tensor streamline tractography in the setting of peritumoral edema and crossing fibers in brain tumor patients.

Keywords

diffusion tensor imaging; corticospinal tract; tractography; peritumoral edema; crossing fibers; neurosurgical planning

Introduction

Diffusion tensor imaging (DTI) is unique in its ability to trace critical fiber pathways *in vivo*, and thus allows for application of neurosurgical planning and intra-operative decision-making [1–6]. However, complex white matter architecture, for example, crossing fibers, a ubiquitous feature of neuroanatomy, poses a major challenge to single-tensor model [7,8]. The single-tensor model fails to account for multiple fibers in a voxel. This inability to resolve multiple intravoxel fiber orientations results in the failure of DTI to trace the subcortical pathway accurately. Conventional DTI techniques depicting the corticospinal tract (CST) actually trace only those fiber tracts that project to the foot area of the cortex and are unable to trace the lateral projections of CST that links to hand- and lip-related functional cortex [9–11]. Moreover, in brain tumor patients, the lesions can dislocate, infiltrate, or destroy the normal course and arrangement of white matter fiber tracts [12–14]. Thus, the challenges of fiber tracking in tumor patients could include effects of peritumoral edema, crossing fibers, infiltration, destruction, or even a combination of effects.

Over the past few years, researchers have proposed several methods to increase the ability of DTI to trace the fiber tracts in complex white matter architecture. Studies have shown that increase of gradient directions, as well as a higher b-value, can be used to resolve the effects of crossing fibers [15,16]. However, the duration of the scan poses an obstacle to its practical clinical applications. Furthermore, the effects of peritumoral edema still impede the correct identification of fiber tracts. Therefore, there is need of a clinically feasible technique that can resolve those challenges.

The two-tensor unscented Kalman filter (UKF) algorithm [17] was designed to perform tractography within a filter framework using a mixture of two Gaussian tensors to model the signal. Each fiber is traced to its termination from a seed point using the filter to simultaneously fit the local model to the signal and propagate in the most consistent direction. This tractography algorithm allows reconstruction of tracts that pass through branching and crossing fiber regions of the human brain. Our previous work has shown that UKF two-tensor tractography can achieve a satisfactory tractography result using clinical scans of 31 directions at a b-value of 1000 s/mm^2 [18].

The aim of this study was to determine whether two-tensor UKF tractography would show improvements in tracing the CST in patients with brain tumors in the vicinity of motor cortex and peritumoral edema.

Materials and Methods

Patient population

We retrospectively evaluated all consecutive brain tumor patients who underwent functional MRI and diffusion imaging at Brigham and Women’s Hospital between December 2008 and April 2011. Patients were selected for inclusion in the current study if they met the following criteria: 1) They were diagnosed with lesions in the vicinity of motor cortex and scheduled for lesion resection; 2) There was significant peritumoral edema surrounding the lesion; 3) The final diagnosis was confirmed by pathology as brain tumor. Exclusion criteria: Any

patient who could not perform the fMRI tasks satisfactorily because of neurological deficits or neurocognitive state. After the exclusion of ineligible subjects, ten patients (2 male, 8 female; age range 32 – 64 years) were chosen for inclusion in our retrospective study. A detailed description of the patients is given in Table 1. The study was approved by the Partners Healthcare Institutional Review Board, and written informed consent was obtained from all subjects prior to participation.

MRI Acquisition

MR images were acquired using a 3-Tesla scanner (EXCITE Signa scanner, GE Medical System, Milwaukee, WI, USA) with Excite 14.0, using an 8-channel head coil and array spatial sensitivity encoding technique (ASSET). High resolution whole brain T1-weighted axial 3D spoiled gradient recalled structural images (TR = 7500 ms, TE = 30 ms, matrix = 512 × 512, FOV = 25.6 cm, FA = 20°, 176 slices, voxel size = 0.5 × 0.5 × 1 mm^3) were obtained.

Diffusion weighted images were obtained using echo-planar imaging (EPI) with 8 channel head coil and ASSET (TR = 14000 ms, TE = 75.4, 31 gradient directions with a b-value of 1000 s/mm^2, 1 baseline image, FOV = 25.6 cm, matrix = 256 × 256, at least 44 slices, voxel size = 2 × 2 × 3 mm^3). Acquisition of diffusion data sets took 7 minutes per patient.

Whole-brain functional images were acquired using a quadrature head coil with single-shot gradient-echo EPI sequence sensitive to the blood-oxygen level dependent (BOLD) signal (TR/TE = 2000/40 ms, FA = 90°, slice gap = 0 mm, FOV = 25.6 cm, in-plane resolution = 128 × 128, voxel size = 2 × 2 × 4 mm^3, ascending interleaved sequence). All the motor tasks were self-paced, blocked designs of alternating 20-second task and rest blocks. The motor paradigms included toe wiggling, hand clenching, finger tapping, and lip pursing. Stimuli were presented using a PC laptop (Dell, Inc., Austin, TX), running the E-prime software package (Psychology Software Tools, Pittsburgh, PA) and projected through MR-compatible goggles (Resonance Technology, Northridge, CA).

Preprocessing of DTI Data

3D Slicer[19] (www.slicer.org, version 4.3) software was used to convert the raw diffusion MRI dataset from DICOM format into NRRD format. We subsequently employed DTIPrep[20] (http://www.nitrc.org/projects/dtiprep) to effect quality control, which included artifact correction/removal as well as eddy-current and head motion artifacts correction by registration to the baseline image. In 3D Slicer, fractional anisotropy (FA) maps were made and the standard color scheme was utilized to visualize the DTI eigenvector orientations (with blue indicating superior–inferior, red indicating transverse, and green indicating anterior–posterior). The DTI tensors were visualized using ellipsoid glyphs in 3D Slicer. All the ten patients' diffusion MRI datasets were analyzed using both single-tensor streamline and two-tensor UKF tractography algorithms.

Single-tensor Streamline Tractography

Single-tensor streamline tractography was achieved in 3D Slicer using the second-order Runge-Kutta (midpoint) method. A binary brain mask was computed in 3D Slicer from the

diffusion images to limit tractography to within the brain. Whole brain tractography was seeded within the brain mask in all voxels where single tensor (standard DTI) FA value was higher than 0.15. Tractography stopped when FA fell below 0.15.

Two-tensor UKF Tractography

The idea of two-tensor UKF tractography approach [17] is to trace the local fiber orientations using the estimation at previous positions to guide estimation at the current position. In a loop, the Kalman filter estimates the model at the current location, moves a step in the most consistent direction, and then begins estimation again. Recursive estimation in this way improves the accuracy of resolving individual orientation and produces inherently smooth tracts despite the noise and uncertainty. The two-tensor UKF tractography was conducted in high performance computing clusters (HPC) and employed to trace whole brain fiber tracts. As in single tensor tractography (above), the tractography was seeded within the binary brain mask in all voxels where single tensor FA value exceeded 0.15, and tractography stopped when FA (of the tensor being tracked) fell below 0.15. In addition to the FA thresholds, the UKF method also uses an additional value, the generalized anisotropy (GA), to further contain tracking within regions where a two-tensor fit is reasonable. Based on the variance of normalized diffusivities, GA is sensitive to the presence of anisotropic features such as fiber crossings. The GA threshold for seeding in the UKF method is 0.18. The GA was also utilized as an additional stopping criterion, and we used the default value of 0.10. The results from whole brain tractography were subsequently imported into 3D Slicer for further analysis.

Fiber Bundle Selection and Volume Measurement

Fiber bundle selection was performed in the 3D Slicer platform. A two-ROI approach [21] was employed in the selection of the CST. The ROIs were determined by a clinically trained neurosurgical research fellow (Z.C.) based on the color-coded FA maps and structural images. The first ROI was drawn on ventral portion of the pons and the other was on the posterior limb of internal capsule. CST volumes were measured as a proxy for its anatomical completeness, as in other studies comparing connections traced by tractography [22]. The Fiber Bundle to Label Map module in 3D Slicer was used to transform the CST into a label map. This module set a specified label value in the label map at every vertex of each of the fibers in each CST. After that, the Label Statistic module was used to calculate the label volume. The volume of the CST was defined as the volume of the voxels occupied by the fibers in each subject.

Functional MRI Analysis

Statistical Parametric Mapping software package (http://www.fil.ion.ucl.ac.uk/spm, SPM8) was used to pre-process and analyze the fMRI data. The functional data were preprocessed with rigid body motion correction by realigning to the session's first functional image, and spatial smoothing using a 6 mm full-width half-maximum (FWHM) Gaussian kernel. We performed the first-level single subject analysis based on the general linear model (GLM) implemented in SPM8. The statistical maps generated from each task design at a threshold of a $p < 0.05$ using a family-wise error (FWE) correction for multiple comparisons. Maps were then imported into 3D Slicer and were subsequently registered to the baseline

diffusion-weighted images using a rigid registration (6 DOF) module [23]. The statistical threshold was finally determined by Z.C. The Save Island function in Edit module was used to select the foot-, hand-, and lip-related ROI maps. After that, we used the Model Maker module to create 3D surface models from fMRI maps for visualization of fMRI activations with fiber tracts.

Statistical Analysis

Statistical analysis was achieved using STATA (version 11.0; StataCorp, College Station, TX, USA). Standard summary statistics were employed to present the volume measurement data. A paired t-test was performed to compare tract volumes across tractography methods. A value of $P < .05$ (two-tailed) was set a priori as the statistically significant level.

Results

The evaluation of the CST was based on quantitative measures of its volume, its relationship to fMRI, and knowledge of neuroanatomy. We have illustrated the differences between single-tensor DTI tractography and two-tensor UKF tractography in four selected cases (Figs. 1 to 5).

Case 1

Figs. 1 to 2 show images from a fifty year old female patient who presented with worsening right upper extremity weakness and potential weakness of her right lower extremity. MRI showed two lesions within the posterior left frontal lobe measuring approximately 1.8 cm × 1.8 cm × 1.2 cm to the inferior lesion and approximately 1.3 cm × 1.1 cm × 1.0 cm per the superior lesion. There was an extensive halo of peritumoral T2 hyperintensity demonstrated on both T2 and FLAIR imaging.

We visualized a region at the border of the lesion (Fig. 1A). Fig. 1B shows that fiber tracts that were reconstructed by single-tensor streamline tractography terminated at the boundary of the edematous area. In contrast, two-tensor UKF tractography tracked some fiber tracts through the edematous area (Fig. 1C). We then visualized the tensors from the standard single-tensor DTI model within the ROI in terms of 3D ellipsoid glyphs. Fig. 1D shows that tensor ellipsoids have a higher eigenvalue magnitude and are nearly spherical within the edematous area, while those within normal white matter have a lower eigenvalue magnitude and demonstrate anisotropy. We found that single-tensor streamline tractography could only trace the fiber tracts when the tensor ellipsoids are apparently anisotropic (Fig. 1E). However, two-tensor UKF tractography showed the ability to trace the fiber tracts in the region even when diffusion was isotropic according to the single-tensor DTI model (Fig. 1F, arrow).

In Fig. 2A, the single-tensor streamline tractography traced only the medial projections of the CST. In contrast, in Fig. 2B, two-tensor UKF tractography tracked lateral projections, producing a fan-shaped fiber bundle which is consistent with the known anatomy of the CST. Meanwhile, the number of tractography fibers in both sides of the lateral projections of CST appeared similar. This suggests that the lateral projections of CST in the diseased hemisphere are not obscured by the effects of peritumoral edema and crossing fibers. Fig.

2C and 2D show the lateral views of results from the two tractography methods. The fiber tracts from single-tensor streamline tractography terminate in the boundary of the edematous area (Fig. 2C). However, two-tensor UKF tractography delineates fiber tracts (arrow) that run through the edema, which appear to be displaced by mass effect when compared to the tracts in the healthy hemisphere. We further compared the relationship between motor fMRI activation and the fiber projections from the two tractography methods. The two-tensor UKF tractography (Fig. 2F and 2H) delineated tracts that were closer to the motor fMRI activation and was more sensitive than single-tensor streamline tractography (Fig. 2E and 2G) to define tracts directed to the motor sites.

Case 2

Fig. 3 shows the images from a 48-year-old man who had been diagnosed with glioblastoma. In Fig. 3A, the lateral projections of CST are not observable on the single-tensor streamline tractography. In contrast, the two-tensor UKF tractography reveals lateral projections of CST (Fig. 3B). Fig. 3C shows the fiber trajectory reconstructed by single-tensor streamline tractography. This image shows that medial projections of CST was disrupted by peritumoral edema. However, two-tensor UKF tractography delineated the fiber tracts which ran through the edematous area (Fig. 3D, arrow). These results suggest a totally different margin for tumor resection. As shown in the figure, it was not possible to reconstruct tracts projecting to fMRI activation of hand (blue model) and lip (purple model) functions with single-tensor streamline tractography (Fig. 3E), but it was possible with two-tensor UKF tractography (Fig. 3F).

Case 3

Fig. 4 shows images from a 32-year-old woman with multiple recurrent glioblastoma multiforme. Her MRI scans showed progressive enlargement of a nonenhancing region in the posterior temporal lobe that extended into the posterior aspect of the right parietal region to the ventricle. The left toe movement task associated BOLD activation was seen over the medial precentral gyrus in the expected location while the left hand clench task associated BOLD activation was seen over the right lateral precentral gyrus in the expected location.

The comparison of two algorithms show that two-tensor UKF tractography tracked (Fig. 4B) an apparently larger CST than single-tensor streamline tractography (Fig. 4A). Fig. 4C and 4E show the results from single-tensor streamline tractography. These results showed that single-tensor model could only trace the medial projections of CST. In contrast, in Fig 4D and 4F, two-tensor UKF tractography traced lateral projections of CST through regions of crossing fibers and peritumoral edema (arrow).

Case 4

Fig. 5 shows images from a 43-year-old woman with a history of metastatic breast cancer. She was initially diagnosed with triple negative breast carcinoma and then developed pulmonary and brain metastases. She had left-sided facial weakness and follow-up brain MRI at that time revealed multiple lesions in the left occipital and right frontal lobes.

Fig. 5 shows that single-tensor streamline tractography underestimated the extent of tracts directed to motor sites (Fig. 5A), whereas two-tensor UKF tractography traced fanning projections of CST (Fig. 5B). In Fig. 5C, using single-tensor streamline algorithm, we found that there were few fiber tracts that linked to hand-related functional cortex and the medial projection appeared to be obscured by the peritumoral edema. In contrast, the two-tensor UKF tractography apparently showed ability to track through regions of edema (Fig. 5D, arrow) and we can see the lateral projections of CST were linked to the hand-related fMRI activation.

Volume analysis

The volumes of the CST from the two-tensor UKF tractography method were significantly greater than those from the single-tensor streamline tractography method (Fig. 6). In our patient dataset (n = 10), the single-tensor streamline group mean (SD) CST volume in mm^3 was 7396.2 (2662.4), while the two-tensor UKF group mean (SD) volume in mm^3 was 79858.9 (13719.5), two-tailed $p < 0.01$. This result suggests that two-tensor UKF tractography traces a larger volume of CST than single-tensor streamline tractography.

Discussion

In this study, we have found that two-tensor UKF tractography could be used to improve the tracking of CST in brain tumor patients by tracking through regions of peritumoral edema and crossing fibers. This has been demonstrated by a comparison of tracking results of single-tensor streamline and two-tensor UKF tractography. Single-tensor streamline tractography underestimated the extent of tracts running through the edematous areas and could only track the medial projections of the CST. In contrast, two-tensor UKF tractography tracked fanning projections of the CST despite peritumoral edema and crossing fibers.

Similar to a previous study [24], our results showed that the single-tensor model did not have the ability to estimate the correct fiber orientation when the image voxel is affected by extracellular water (the phenomenon also called partial volume effect). Another single-tensor model limitation is the fiber crossing issue [9,15,16,25], the well-known reason why single-tensor streamline tractography can only trace the medial projections of CST. In this study, two-tensor UKF tractography overcame the limitations of single-tensor model. The two-tensor model provided a better estimate than the single-tensor model when facing complex white matter structures such as edema-affected fiber tracts and crossing fibers.

Other methods have been proposed to improve the fiber tracking through regions of edema and/or crossing fibers. Mandelli et al [26] performed a clinical study to quantify accuracy and precision of diffusion MR tractography of the CST in brain tumors. Their results showed that a probabilistic tracking method delineated tracts that were significantly closer to stimulation points and was more sensitive than a deterministic DTI method in defining the tracts that were directed to the motor sites. However, both DTI techniques demonstrated poor sensitivities to finding lateral motor regions. Our study and theirs showed that higher-order diffusion model tractography could be used to address the challenge of crossing fibers. However, their study didn’t provide evidence that probabilistic tracking is suitable for

tracing through edema. Diffusion spectrum imaging[16] and Q-ball imaging[15] are both novel techniques that demonstrate the ability to resolve the challenges of complex intravoxel fiber architecture. They offer a more complete and more accurate representation of the true diffusion function. However, measuring the complete three-dimensional diffusion function requires long acquisition times and strong magnetic field gradients. This is an obstacle to mapping the fiber matter pathway in the clinical setting. As we demonstrated in our study, clinical diffusion data of around 30 directions at a b-value of 1000 s/mm^2 is adequate for two-tensor UKF tractography. Another study by Zhang et al [27] showed that generalized q-sampling imaging can visualize the tracts in the peritumoral edema of cerebral tumors better than DTI. McDonald et al [28] also demonstrated that restriction spectrum imaging can be used to improve the quantification and visualization of white matter tracts in regions of peritumoral edema. As in our study of two-tensor UKF tractography, all these methods showed some extent of improvement of tracing through edema.

In this study, using the same ROIs for fiber bundle selection, two-tensor UKF tractography traced a much larger volume of CST than single-tensor streamline tractography. On the one hand, this result showed that two-tensor UKF tractography was more robust than single-tensor streamline tractography, but on the other hand, as we know, not all of these fiber tracts were related to motor function (especially a few fiber tracts were located in the frontal and/or occipital lobes). It is essential to identify the motor-related functional fiber tracts [29,30]. In our work, we used the motor task fMRI to increase the specificity (identify the functional fiber tracts). Also, this study was a small cohort of patients who were mainly composed by high grade glioma. High grade glioma is a very aggressive pathological process and the T2 bright signal surrounding glioma can be attributed not only to increased water content, but also tumor cell infiltration [31]. In our study, we only indicated that UKF tractography could be used to improve the tracing through edema as it was more confident to define edema than tumor cell infiltration.

Tracking the critical functional fiber tracts by addressing the effects of peritumoral edema and crossing fibers is crucial for neurosurgical planning for resection of lesions in the vicinity of motor cortex [26]. Our results showed that single-tensor streamline tractography displays incomplete fiber tracts and tends to provide a greater safe resection margin. This inaccurate information could result in severe post-operative neurologic deficits. Accurate estimation of fiber tracts would provide valuable information for neurosurgeon to define a safe resection margin when trying to achieve the goal of “total resection.” Two-tensor UKF tractography may be an alternative method but further validation is needed.

Limitations

First, the two-tensor UKF tractography algorithm is more computationally intensive than the single-tensor streamline tractography method. The procedure for single-tensor streamline whole brain tractography required 5 to 10 minutes for each subject on a desktop computer while two-tensor UKF tractography required up to 20 minutes in the HPC, or up to 60 to 120 minutes to run per patient on a regular desktop. Second, although the two-tensor UKF tractography tracked a larger volume of CST than single-tensor streamline tractography, because there is no gold standard for validation (such as direct electrical stimulation) in this

study, the possibility of false positives and/or false negatives should be taken into account. Third, as a retrospective study, there is no comparison of postoperative outcomes between the single-tensor streamline and two-tensor UKF approaches. Further studies will require a larger sample size and direct cortical stimulation to further validate the ability of two-tensor UKF algorithm in fiber tracking.

Conclusion

In this study, we have found that two-tensor UKF tractography could be used to improve the tracking of CST in brain tumor patients by tracking through regions of peritumoral edema and crossing fibers. The improved tracking of CST may help the neurosurgeons to define a safe resection margin more accurately when trying to achieve the goal of total resection. Although two-tensor UKF tractography has shown promise, effectiveness of this algorithm needs further validation.

Acknowledgments

National Institutes of Health (R21CA156943, P41EB015898, R21NS075728) to A.J.G.; National Institutes of Health (P41EB015902, R01MH074794, R21CA156943, P41EB015898, U01NS083223) to L.J.O.; National Institutes of Health (R01MH097979) to Y.R.; National Institutes of Health (P41EB015902, R01MH074794) to O.P.; The Brain Science Foundation to Y.T.; Oversea Study Program of Guangzhou Elite Project to Z.C.

References

1. Golby AJ, Kindlmann G, Norton I, Yarmarkovich A, Pieper S, Kikinis R. Interactive diffusion tensor tractography visualization for neurosurgical planning. Neurosurgery. 2011; 68(2):496–505. [PubMed: 21135713]
2. Kamada K, Sawamura Y, Takeuchi F, Kawaguchi H, Kuriki S, Todo T, Morita A, Masutani Y, Aoki S, Kirino T. Functional identification of the primary motor area by corticospinal tractography. Neurosurgery. 2005; 56(1 Suppl):98–109. discussion 198-109. [PubMed: 15799797]
3. Castellano A, Bello L, Michelozzi C, Gallucci M, Fava E, Iadanza A, Riva M, Casaceli G, Falini A. Role of diffusion tensor magnetic resonance tractography in predicting the extent of resection in glioma surgery. Neuro-oncology. 2012; 14(2):192–202. [PubMed: 22015596]
4. Bello L, Gambini A, Castellano A, Carrabba G, Acerbi F, Fava E, Giussani C, Cadioli M, Blasi V, Casarotti A, Papagno C, Gupta AK, Gaini S, Scotti G, Falini A. Motor and language DTI Fiber Tracking combined with intraoperative subcortical mapping for surgical removal of gliomas. NeuroImage. 2008; 39(1):369–382. [PubMed: 17911032]
5. Shahar T, Rozovski U, Marko NF, Tummala S, Ziu M, Weinberg JS, Rao G, Kumar VA, Sawaya R, Prabhu SS. Preoperative imaging to predict intraoperative changes in tumor-to-corticospinal tract distance: an analysis of 45 cases using high-field intraoperative magnetic resonance imaging. Neurosurgery. 2014; 75(1):23–30. [PubMed: 24618800]
6. Trope M, Shamir RR, Joskowicz L, Medress Z, Rosenthal G, Mayer A, Levin N, Bick A, Shoshan Y. The role of automatic computer-aided surgical trajectory planning in improving the expected safety of stereotactic neurosurgery. International journal of computer assisted radiology and surgery. 2014
7. Basser PJ, Pajevic S, Pierpaoli C, Duda J, Aldroubi A. In vivo fiber tractography using DT-MRI data. Magnetic resonance in medicine : official journal of the Society of Magnetic Resonance in Medicine / Society of Magnetic Resonance in Medicine. 2000; 44(4):625–632.
8. Nimsky C. Fiber Tracking-We Should Move Beyond Diffusion Tensor Imaging. World neurosurgery. 2013

9. Farquharson S, Tournier JD, Calamante F, Fabinyi G, Schneider-Kolsky M, Jackson GD, Connelly A. White matter fiber tractography: why we need to move beyond DTI. Journal of neurosurgery. 2013; 118(6):1367–1377. [PubMed: 23540269]
10. Bucci M, Mandelli ML, Berman JI, Amirbekian B, Nguyen C, Berger MS, Henry RG. Quantifying diffusion MRI tractography of the corticospinal tract in brain tumors with deterministic and probabilistic methods. NeuroImage Clinical. 2013; 3:361–368. [PubMed: 24273719]
11. Qazi AA, Radmanesh A, O'Donnell L, Kindlmann G, Peled S, Whalen S, Westin CF, Golby AJ. Resolving crossings in the corticospinal tract by two-tensor streamline tractography: Method and clinical assessment using fMRI. NeuroImage. 2009; 47(Suppl 2):T98–T106. [PubMed: 18657622]
12. Schonberg T, Pianka P, Hendler T, Pasternak O, Assaf Y. Characterization of displaced white matter by brain tumors using combined DTI and fMRI. NeuroImage. 2006; 30(4):1100–1111. [PubMed: 16427322]
13. Kinoshita M, Yamada K, Hashimoto N, Kato A, Izumoto S, Baba T, Maruno M, Nishimura T, Yoshimine T. Fiber-tracking does not accurately estimate size of fiber bundle in pathological condition: initial neurosurgical experience using neuronavigation and subcortical white matter stimulation. NeuroImage. 2005; 25(2):424–429. [PubMed: 15784421]
14. Clark CA, Barrick TR, Murphy MM, Bell BA. White matter fiber tracking in patients with space-occupying lesions of the brain: a new technique for neurosurgical planning? NeuroImage. 2003; 20(3):1601–1608. [PubMed: 14642471]
15. Tuch DS, Reese TG, Wiegell MR, Wedeen VJ. Diffusion MRI of complex neural architecture. Neuron. 2003; 40(5):885–895. [PubMed: 14659088]
16. Wedeen VJ, Wang RP, Schmahmann JD, Benner T, Tseng WY, Dai G, Pandya DN, Hagmann P, D'Arceuil H, de Crespigny AJ. Diffusion spectrum magnetic resonance imaging (DSI) tractography of crossing fibers. NeuroImage. 2008; 41(4):1267–1277. [PubMed: 18495497]
17. Malcolm JG, Shenton ME, Rathi Y. Filtered multitensor tractography. IEEE transactions on medical imaging. 2010; 29(9):1664–1675. [PubMed: 20805043]
18. Baumgartner C, Michailovich O, Levitt J, Pasternak O, Bouix S, Westin C, Rathi Y. A unified tractography framework for comparing diffusion models on clinical scans. CDMRI Workshop–MICCAI, Nice. 2012
19. Gering DT, Nabavi A, Kikinis R, Hata N, O'Donnell LJ, Grimson WE, Jolesz FA, Black PM, Wells WM 3rd. An integrated visualization system for surgical planning and guidance using image fusion and an open MR. Journal of magnetic resonance imaging : JMRI. 2001; 13(6):967–975. [PubMed: 11382961]
20. Liu Z, Wang Y, Gerig G, Gouttard S, Tao R, Fletcher T, Styner M. Quality Control of Diffusion Weighted Images. Proceedings - Society of Photo-Optical Instrumentation Engineers. 2010; (7628)
21. Mori S, van Zijl PC. Fiber tracking: principles and strategies - a technical review. NMR in biomedicine. 2002; 15(7–8):468–480. [PubMed: 12489096]
22. Propper RE, O'Donnell LJ, Whalen S, Tie Y, Norton IH, Suarez RO, Zollei L, Radmanesh A, Golby AJ. A combined fMRI and DTI examination of functional language lateralization and arcuate fasciculus structure: Effects of degree versus direction of hand preference. Brain and cognition. 2010; 73(2):85–92. [PubMed: 20378231]
23. Johnson H, Harris G, Williams K. BRAINSFit: mutual information rigid registrations of whole-brain 3D images, using the insight toolkit. Insight J. 2007
24. Pasternak O, Sochen N, Gur Y, Intrator N, Assaf Y. Free water elimination and mapping from diffusion MRI. Magnetic resonance in medicine : official journal of the Society of Magnetic Resonance in Medicine / Society of Magnetic Resonance in Medicine. 2009; 62(3):717–730.
25. Peled S, Friman O, Jolesz F, Westin CF. Geometrically constrained two-tensor model for crossing tracts in DWI. Magnetic resonance imaging. 2006; 24(9):1263–1270. [PubMed: 17071347]
26. Mandelli ML, Berger MS, Bucci M, Berman JI, Amirbekian B, Henry RG. Quantifying accuracy and precision of diffusion MR tractography of the corticospinal tract in brain tumors. Journal of neurosurgery. 2014; 121(2):349–358. [PubMed: 24905560]
27. Zhang H, Wang Y, Lu T, Qiu B, Tang Y, Ou S, Tie X, Sun C, Xu K, Wang Y. Differences between generalized q-sampling imaging and diffusion tensor imaging in the preoperative visualization of

the nerve fiber tracts within peritumoral edema in brain. Neurosurgery. 2013; 73(6):1044–1053. discussion 1053. [PubMed: 24056318]

28. McDonald CR, White NS, Farid N, Lai G, Kuperman JM, Bartsch H, Hagler DJ, Kesari S, Carter BS, Chen CC, Dale AM. Recovery of white matter tracts in regions of peritumoral FLAIR hyperintensity with use of restriction spectrum imaging. AJNR American journal of neuroradiology. 2013; 34(6):1157–1163. [PubMed: 23275591]
29. Conti A, Raffa G, Granata F, Rizzo V, Germano A, Tomasello F. Navigated transcranial magnetic stimulation for "somatotopic" tractography of the corticospinal tract. Neurosurgery. 2014; 10(Suppl 4):542–554. discussion 554. [PubMed: 25072115]
30. Berman JI, Berger MS, Mukherjee P, Henry RG. Diffusion-tensor imaging-guided tracking of fibers of the pyramidal tract combined with intraoperative cortical stimulation mapping in patients with gliomas. Journal of neurosurgery. 2004; 101(1):66–72. [PubMed: 15255253]
31. Lu S, Ahn D, Johnson G, Cha S. Peritumoral diffusion tensor imaging of high-grade gliomas and metastatic brain tumors. AJNR American journal of neuroradiology. 2003; 24(5):937–941. [PubMed: 12748097]

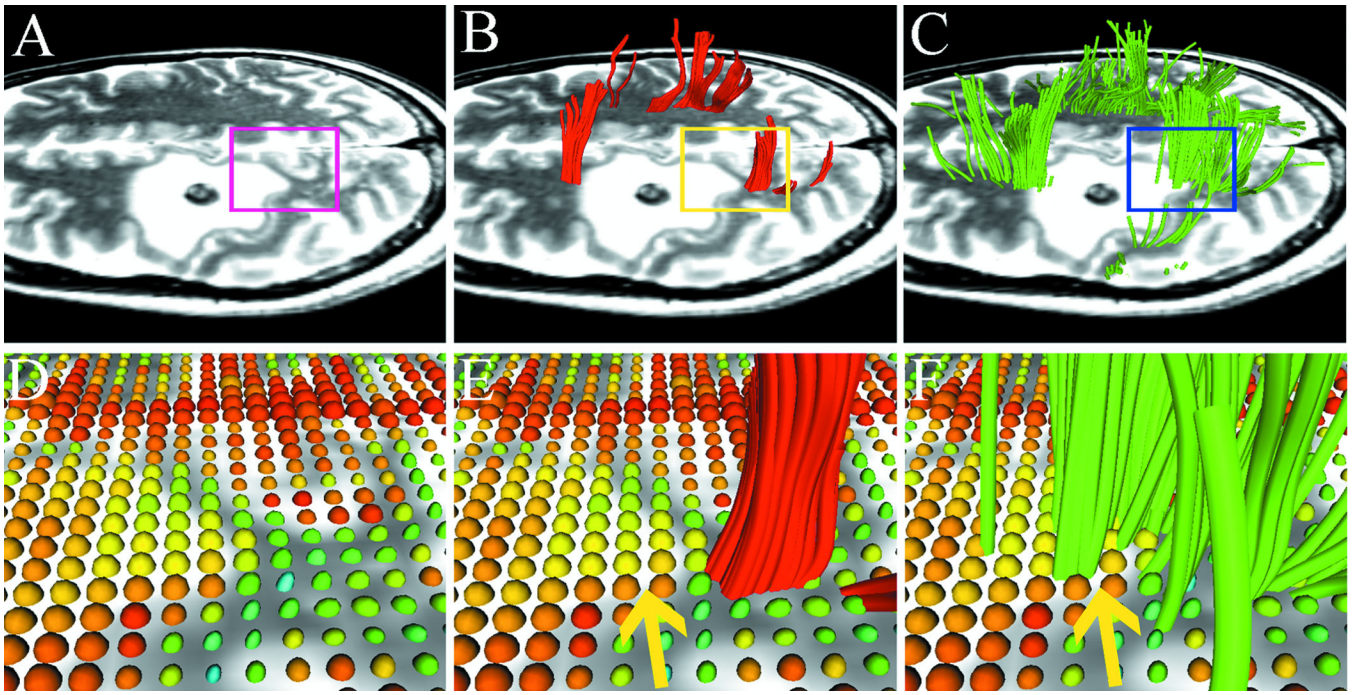

Fig. 1.

Results from case 1 with left frontal metastatic sarcoma. T2-weighted images demonstrate a lesion with significant peritumoral edema and a region-of interest (ROI) is placed on the boundary of the lesion (A) to specify the zoomed-in region (bottom row). Using single-tensor streamline tractography (red fibers), there is no fiber tract that runs through the edematous area (B). Two-tensor unscented Kalman filter (UKF) tractography (green) shows tracing of corticospinal tract (CST) portions that run through the edematous area (C). 3D ellipsoid glyphs show the diffusion tensor model (DTI) in the ROI (D), where isotropic diffusion is shown by red and orange glyph colors. Single-tensor streamline tractography traced fiber tracts only where the tensor ellipsoids are apparently anisotropic (E). In contrast, two-tensor UKF tractography could track in regions with isotropic diffusion (F, arrow).

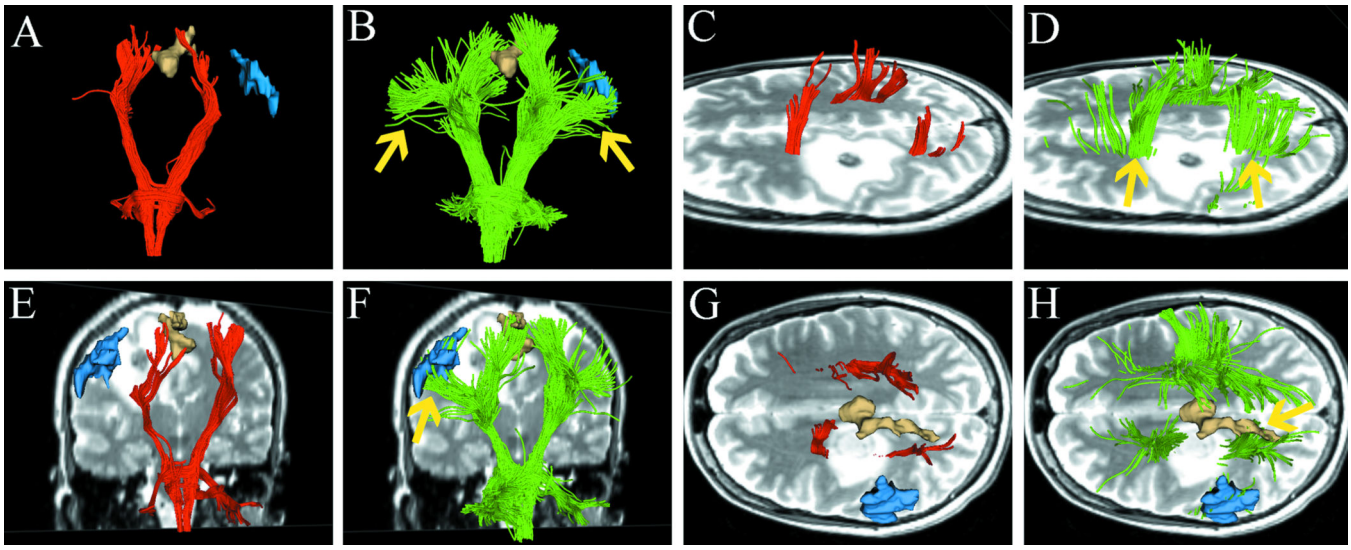

Fig. 2.

Case 1 tractography results versus fMRI. Images show single-tensor tractography in red, two-tensor UKF tractography in green, and fMRI motor activations of foot (tan) and hand (blue). (A) and (B) show the comparison of tracking results between the methods, where more lateral projections are found by the UKF method (arrows). (C) and (D) show the lateral views of tracking results, where UKF tractography delineates some fiber tracts (arrow) that run through the edema. The correlation between motor fMRI activation and the fiber projections from the two tractography methods is shown in (E–H). Single-tensor streamline does not connect with fMRI activation of hand function (E). In contrast, the lateral projections of CST reconstructed by two-tensor UKF tractography are connected to the activation of hand function (F, arrow). In the superior view, although single-tensor streamline tractography shows some correlation between the medial projections of CST and fMRI activation of foot function (G), the two-tensor UKF tractography demonstrates a better correlation between foot function and fiber tracts (H, arrow).

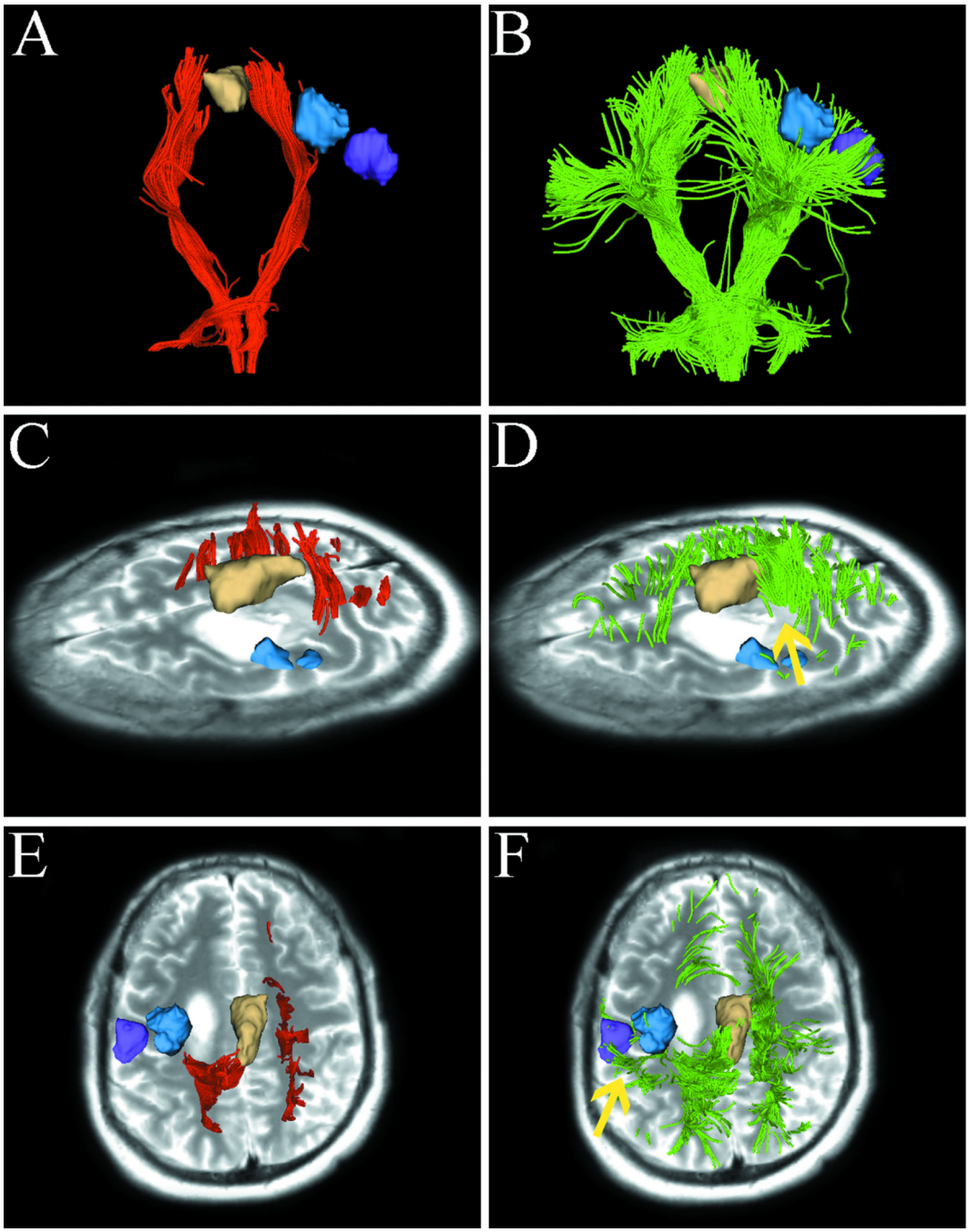

Fig. 3.

Images from case 2 with a left frontal glioblastoma. Images show single-tensor tractography in red, two-tensor UKF tractography in green, and fMRI motor activations of foot (tan), hand (blue), and lip (purple). (A) and (B) show the comparison of tracking results between single-tensor streamline and two-tensor UKF tractography. (C) shows the medial projections of CST which appear to be disrupted because single-tensor streamline tractography underestimates the tracts passing through edema. However, two-tensor UKF tractography delineated some fiber tracts running through the edematous area (D, arrow). The superior

views of the results from two different methods are illustrated in (E) and (F), showing that two-tensor UKF tractography better tracked the lateral projections of CST that projected to hand- and lip-related functional cortex (arrow).

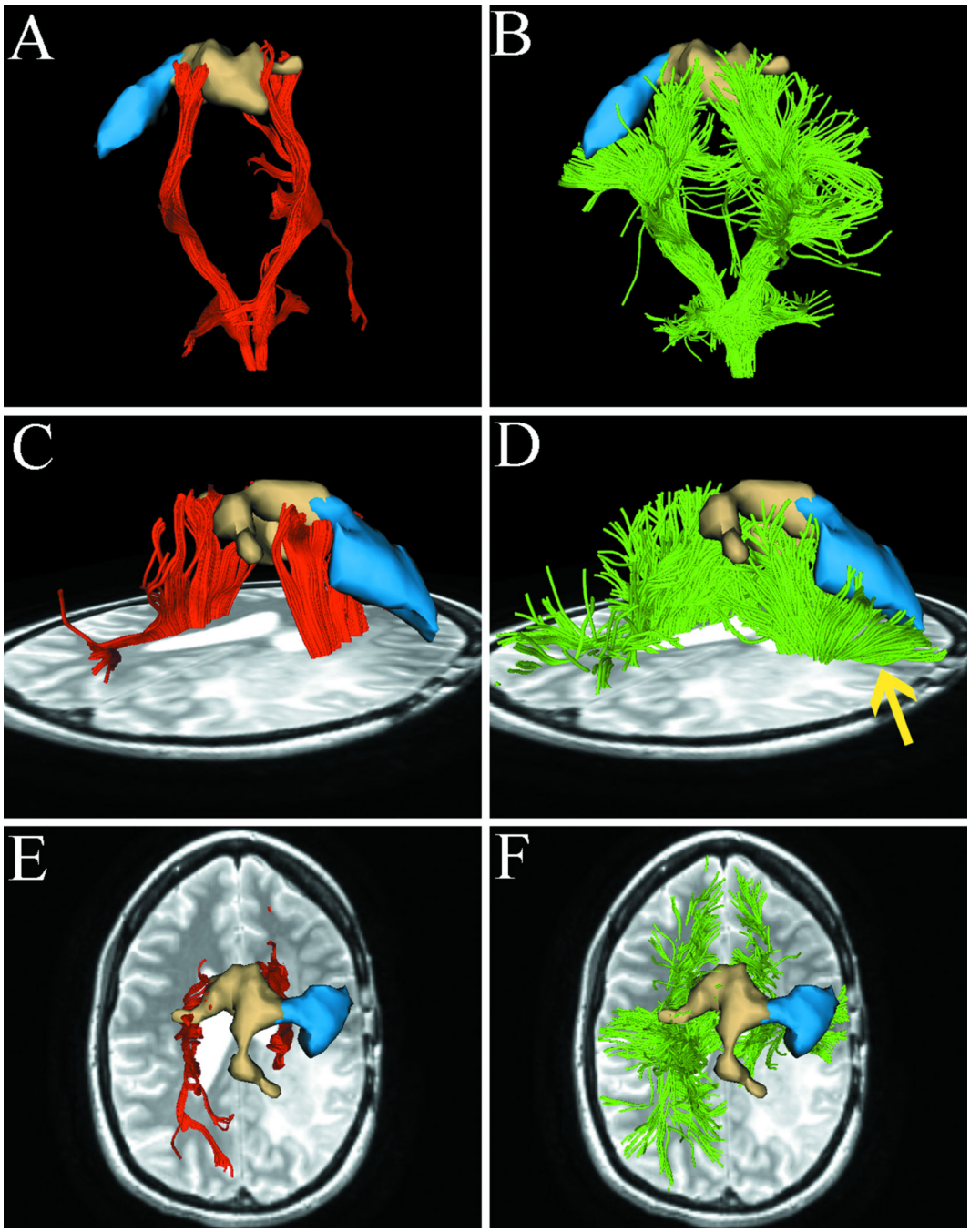

Fig. 4.

Images from case 3 with recurrent glioblastoma. Images show single-tensor tractography in red, two-tensor UKF tractography in green, and fMRI motor activations of foot (tan) and hand (blue). In contrast to the single-tensor results (left column A, C, E), two-tensor UKF tractography traced the lateral projections of CST through regions of crossing fibers and peritumoral edema (B, D, and F, arrow).

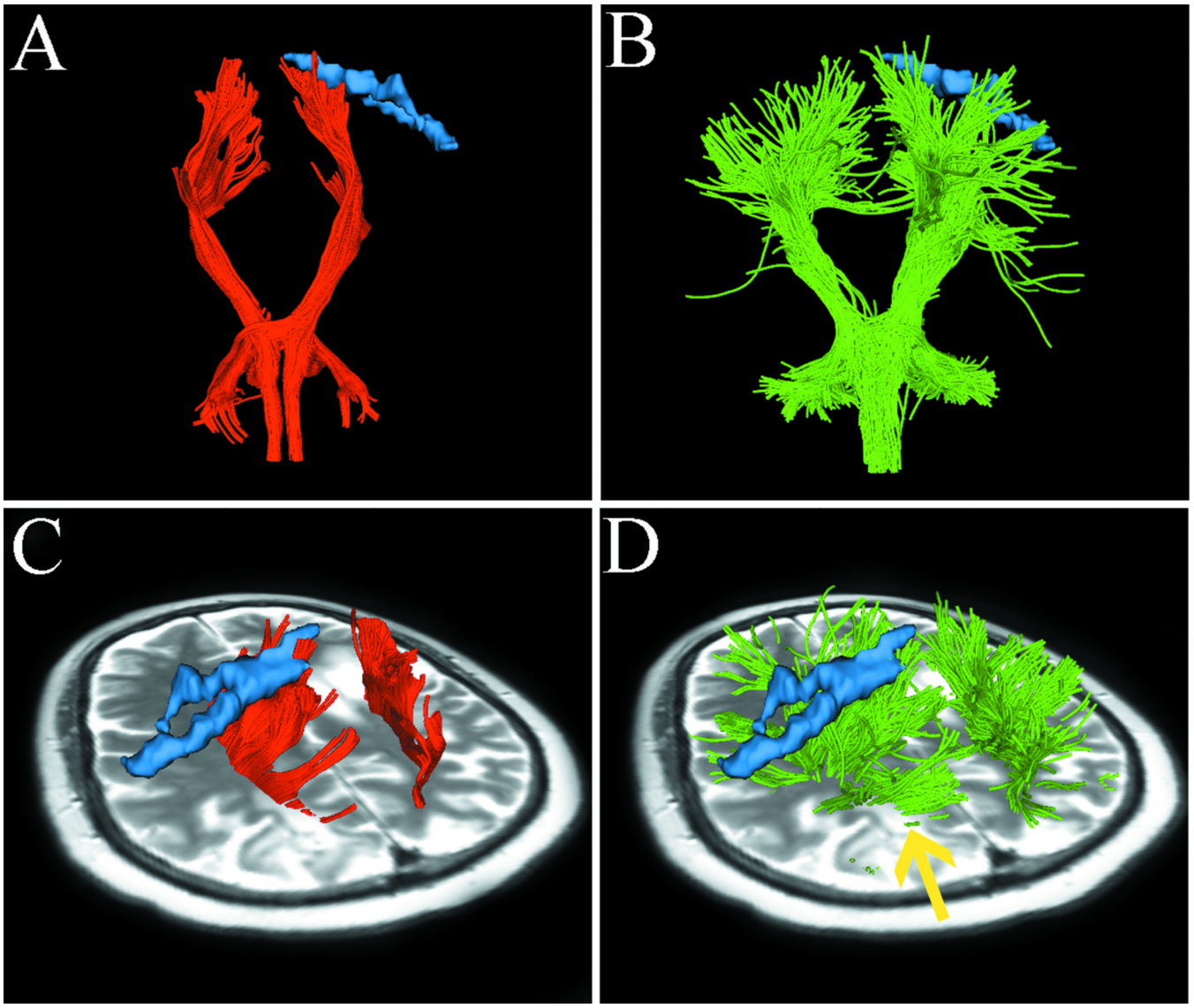

Fig. 5.

Images from case 5 with metastatic breast cancer. Images show single-tensor tractography in red, two-tensor UKF tractography in green, and fMRI motor activations of hand (blue). The lesion of interest for surgical planning and peritumoral edema are indicated by the arrow (D). (A) and (B) show that single-tensor streamline tractography underestimated the tracking of the lateral projections of CST (red), whereas two-tensor UKF tractography traced fanning projections of CST (green). Using the single-tensor streamline algorithm, we found that few fiber tracts linked to hand-related functional cortex and the medial projection appeared to be obscured by the peritumoral edema (C). In contrast, the two-tensor UKF tractography apparently showed the ability to track through regions of edema and the lateral projections of CST which were linked to the hand-related fMRI activation (D, arrow).

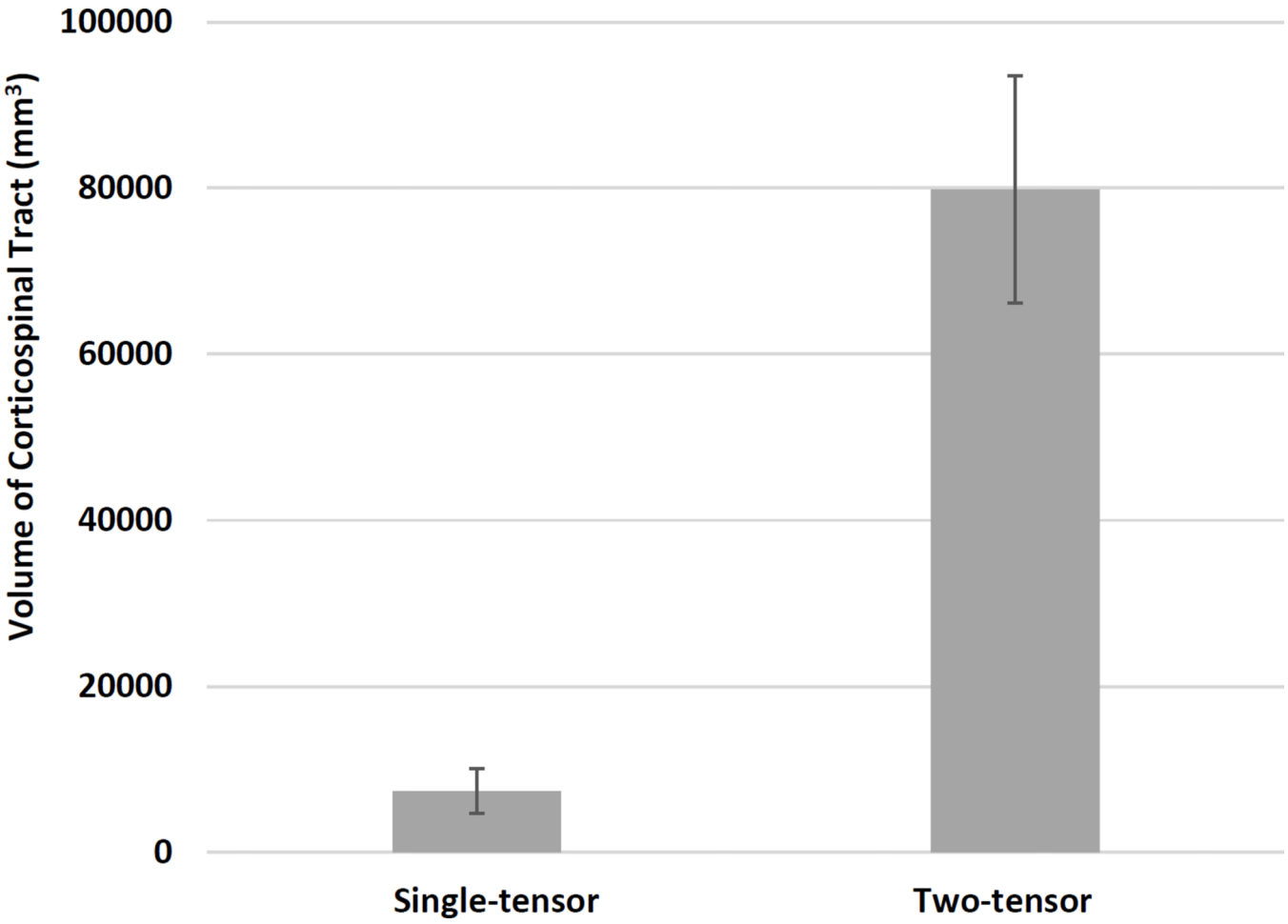

Fig. 6.

Bar graph showing a significant difference between the volumes of the CST as measured by single-tensor streamline and two-tensor UKF tractography methods, n = 10, $p < 0.001$, two-tailed paired t-test.

Table 1

Patient Demographics

Case	Age (years)	Sex	Presentation	Pathology	Localization
1	50	F	Right extremity weakness	Metastatic sarcoma	Left frontal
2	48	M	Seizures	Glioblastoma, WHO IV	Left frontal
3	32	F	Mild focal seizures	Recurrent glioblastoma, WHO IV	Right temporal
4	43	F	Left facial weakness	Multiple metastatic breast cancer	Left occipital and right frontal
5	54	F	Facial twitching, seizures	Glioblastoma, WHO IV	Left fronto-parietal
6	62	F	Dysarthria, right hand clumsiness	B cell lymphoma	Left parietal
7	53	F	Intermittent sensory symptoms	Anaplastic oligodendroglioma, WHO III	Right parietal
8	62	F	Facial droop, left arm weakness	Anaplastic oligodendroglioma, WHO III	Right frontal
9	43	M	Seizures	Anaplastic oligodendroglioma, WHO III	Right parietal
10	64	F	Headaches	Recurrent glioblastoma, WHO IV	Right parietal

WHO, World Health Organization